Egypt. J. Chem. **Vol. 65,** No. SI13B pp. 1489 - 1505 (2022)

Egyptian Journal of Chemistry

http://ejchem.journals.ekb.eg/

Design, Synthesis and Biological Evaluation of Novel Pyrano[2,3-c]pyrazoles And Their Sugar Derivatives as Antimicrobial, Antioxidant and Anticancer Agents

Ibrahim F. Nassar[1*], Hadeer M. El Fekey[2], Zeinab Hamza[3], Heba M. Abo-Salem[4], Adel A.-H. Abdel-Rahman [2]

*[*1]Faculty of Specific Education, Ain Shams University, Abassia, Cairo, Egypt;*

[2]Chemistry Department, Faculty of Science, Menoufia University, Shebin El-Kom, Egypt;

[3]Food Toxicology and Contaminants Department, National Research Centre, Dokki, Giza, Egypt; [4]Chemistry of Natural Compounds Department, Pharmaceutical and Drug Industries Research Institute, NRC

Abstract

Treatment of 2,5-Diphenyl-2,4-dihydro-pyrazol-3-one (1) with 2-Chloro-benzaldehyde (2) in ethanol/sodium hydroxide solution afforded the chalcone derivative (3) which was reacted with malononitrile to afford 6-Amino-4-(2-chloro-phenyl)-1,3-diphenyl-1,4-dihydro-pyrano[2,3-c] pyrazole-5-carbonitrile (4). Compound 4 was reacted with formic acid, acetic anhydride, formamide, thiourea, urea, conc. cold sulfuric acid, D-glucose, p-methoxy benzaldehyde, 4-dimethyl aminobenzaldehyde, benzoyl chloride, triethyl orthoformate to afford a series of pyranopyrazole derivatives (5-15). The formimidic acid ethyl ester 15 was reacted with hydrazine hydrate to afford 4-(2-chlorophenyl)-5-imino-1,3-diphenyl-1,4-dihydropyrazolo[4',3':5,6]pyrano[2,3-d]pyrimidin-6(5H)-amine (16). Compound 16 was then reacted with D-xylose to afford the sugar derivative 17. Also compound 16 was reacted with CS2 to afford 18 in a good yield. Evaluation of the antimicrobial, antioxidant and anticancer Activities of the newly synthesized compounds was performed with a Docking study.

Keywords: Pyranopyrazole, Antimicrobial, Antioxidant, Anticancer, Docking.

1. Introduction

4H-Pyrans belongs to an important class of heterocyclic compounds due to their wide biological and pharmaceutical properties, such as diuretic, spasmolytic, anticancer, anti-coagulant , antitumor [1], antimicrobial [2], mutagenicity [3], antiviral, anti-proliferative. Furthermore, these compounds can be used for the treatment of schizophrenia, Alzheimer's disease and myoclonus diseases [4]. In addition, 4H-Pyran is a constituent of some natural products and several 2-amino-4H-Pyrans are useful as photoactive materials. Also, the antifungal and anti-TB activities of some 4H-Pyrans with different substitutions as a novel pharmacophore have also been investigated [5].

On the other hand, Pyranopyrazole compounds, oxygen- and nitrogen-ring fused heterocycles, are important group of heterocyclic compounds with natural and synthetic molecules [6]. The synthesis of the heterocyclic compounds containing the pyranopyrazole moiety is of great importance, besides its biological and medicinal properties. Pyranopyrazoles have attracted the attention in agrochemical research due to their fungicidal, bactericidal, and herbicidal properties. There are four isomeric structures for pyranopyrazole including: pyrano[2,3-c]pyrazole, pyrano[3,2-c]pyrazole, pyrano[3,4-c]pyrazole, and pyrano[4,3-c]pyrazole, but pyrano[2,3-c]pyrazole isomer is the most investigated one, on the other hand, reports on the preparation of other three pyranopyrazoles are rare [7]. Pyranopyrazoles have important roles based on their biological activity, which includes anti-inflammation [8] and insecticidal effects, [9] besides being identified as a screening kit for the Chk1 kinase inhibitor. Different methods have been reported [11–18] for the synthesis of these derivatives.

From the above facts and in continuation of our previous studies for synthesizing and design of novel heterocyclic and their sugar containing derivatives used as potent, selective and anticancer candidates [19-33] of low toxicity. In the regard to the broad spectrum of biological activities associated with pyrazoles we herein report the synthesis of new pyrano[2,3-c]pyrazole derivatives and their sugar derivatives and screen them in vitro for their antimicrobial, antioxidant, and anticancer activities. Moreover, Docking studies were carried out to

*Corresponding author e-mail: dr.ibrahim.nassar@sedu.asu.edu.eg

Receive Date: 06 June 2022, Revise Date: 11 June 2022, Accept Date: 12 June 2022

DOI: 10.21608/EJCHEM.2022.143253.6253

©2022 National Information and Documentation Center (NIDOC)

understand the pharmaceutical potency of the compounds.

2.Materials and methods

Experimental

Chemistry

All melting points were measured using a Reichert Thermovar apparatus (Reichert Technologies, Depew, NY) and are uncorrected. The Yields listed are of isolated compounds. The IR spectra were recorded on a PerkinElmer model 1720 FTIR spectrometer (PerkinElmer, Waltham, MA) for KBr disc. 1H NMR and 13C NMR were recorded on Bruker (400 MHz) spectrometer using deuterated dimethyl sulfoxide or chloroform as solvents. The data were reported as chemical shifts or δ values (ppm) relative to tetramethylsilane (TMS) as the internal standard and the coupling constants J values are given in Hz. Signals were indicated by the following abbreviations: s = singlet, d = doublet, t = triplet, q = quartet and m = multiplet.

All chemicals and solvents were purchased from commercialsch suppliers. IR, 1H NMR, 13C NMR and elemental analyses were performed at the Micro analytical center at the Faculty of Science, Cairo University, Cairo, Egypt.

4-(2-Chloro-benzylidene)-2,5-diphenyl-2,4-dihydro-pyrazol-3-one (3)

To a solution of 2,5-Diphenyl-2,4-dihydro-pyrazol-3-one (1) (2.36 g, 0.01 mol) in ethanol (50 mL), 2-chloro benzaldehyde (2) (1.125 ml, 0.01 mol) was added with stirring of the previous mixture. NaOH (20%, 15 mL) was added portion wise and stirring was continued for 24 hours. The product was poured into ice then neutralize with dil. HCl. The obtained precipitate was filtered off, dried, and recrystallized from benzene to give 3 as beige crystals; yield 92%; m.p.118-120℃; IR (KBr): ύ /cm^{-1}: 3061, 2937 (CH), 1712 (C=O), ^{1}H-NMR (DMSO-d$_6$) (δ ppm): 7.20 (m, 2H, Ar-H), 7.28 (m, 3H, Ar-H), 7.35 (m, 5H, Ar-H),7.45 (m, 2H, Ar-H), 7.79-7.81 (m, 3H, C=CH, Ar-H), Analysis Calcd. For $C_{22}H_{15}ClN_2O$ (358.82) C, 73.64; H, 4.21; N, 7.81; Found: C, 73.70; H, 4.19; N, 7.85.

6-Amino-4-(2-chloro-phenyl)-1,3-diphenyl-1,4-dihydro-pyrano[2,3-c] pyrazole-5-carbonitrile (4)

A mixture of compound **3** (3.58g, 0.01mol) and malononitrile (0.66g, 0.01mol) in absolute ethanol (30 ml) was refluxed for 4 hours. The solution was cooled at room temperature. Excess ethanol was evaporated under the vacuum. The precipitated solid was recrystallized from ethyl acetate to produce compound **4** as brown crystals; yield 80%; m.p.123-125℃; IR (KBr): ύ /cm^{-1}: 3310 (NH_2), 2188 (CN), 1660 (C=O), ^{1}H-NMR (DMSO-d6) (δ ppm): 4.50 (s, CH, pyran-CH), 6.80 (s, 1H, NH_2 exchangeable), 7.20 (m, 2H, Ar-H), 7.28 (m, 3H, Ar-H), 7.35 (m, 5H, Ar-H),7.45 (m, 2H, Ar-H), 7.79-7.81 (m, 2H, Ar-H), MS m/z: 426 (32%), 424 (100.0%), 256.12 (14.2%), Analysis Calcd. For $C_{25}H_{17}ClN_4O$ (424.89) C, 70.67; H, 4.03; N, 13.19; Found: C, 70.70; H, 4.21; N, 13.10.

4-(2-chlorophenyl)-1,3-diphenyl-4,6,7,8-tetrahydropyrazolo[4',3':5,6] pyrano[2,3-d]pyrimidin-5(1H)-one (5)

A mixture of compound **4** (2.12 g, 5 mmol) and formic acid (20 mL) was refluxed for 2 hours, the reaction mixture was poured after cooling into water and crushed ice, the solid formed was filtered off, washed with cold water and crystallized from ethanol to give **5** as light brown crystals; yield 63 %; m.p.100-102℃; IR (KBr): ύ /cm^{-1}: 3193, 3163 (NH), 1711 (C=O), ^{1}H-NMR (DMSO-d$_6$) (δ ppm): 1.40 (s, 1H, NH exchangeable), 4.50 (s, CH, pyran-CH), 7.20 (m, 2H, Ar-H), 7.28 (m, 3H, Ar-H), 7.35 (m, 5H, Ar-H),7.45 (m, 2H, Ar-H), 7.79-7.81 (m, 2H, Ar-H), 8.60 (s, 1H, NH exchangeable); ^{13}C-NMR (DMSO-d$_6$) (δ ppm): 33 (CH), 45 (CH_2), 85(C-NH), 120- 150 (Ar-C), 170 (C=O); Analysis Calcd. For $C_{26}H_{19}ClN_4O_2$ (454.91) C, 68.65; H, 4.21; N, 12.32; Found: C, 68.70; H, 4.15; N, 12.30.

4-(2-chlorophenyl)-7-methyl-1,3-diphenyl-1,4-dihydro-5H-pyrazolo[4',3':5,6] pyrano [2,3-d][1,3]oxazin-5-one (6)

A solution of **4** (2.12g, 5 mmol) and acetic anhydride (20 ml) was refluxed on a hot plate for 8 hours, excess of acetic anhydride was removed using rotatory evaporator. the solid removed after evaporation was crystallized from petroleum ether to give **6** as brown crystals; yield 93%; m.p.133-135℃; ^{1}H-NMR (DMSO-d6) (δ ppm): 1.20 (s, 3H,CH_3), 4.50 (s, CH, pyran-CH), 7.20 (m, 2H, Ar-H), 7.28 (m, 3H, Ar-H), 7.35 (m, 5H, Ar-H),7.45 (m, 2H, Ar-H), 7.79-7.81 (m, 2H, Ar-H); Analysis Calcd. For $C_{27}H_{18}ClN_3O_3$ (467.90) C, 69.31; H, 3.88; N, 8.98; Found: C, 69.25; H, 3.87; N, 8.99.

4-(2-chlorophenyl)-1,3-diphenyl-1,4-dihydropyrazolo[4',3':5,6]pyrano[2,3-d]pyrimidin-5-amine (7)

A mixture of **4** (2.12g, 5mmol) and formamide (10 mL) was refluxed with stirring at 100^o C for 2 hours. the reaction mixture was poured after cooling into water and crushed ice; the solid formed was filtered off, washed with cold water and crystallized from xylene to give **7** as black crystals; yield 74%; m.p.114-116℃; IR (KBr): ύ /cm^{-1}: 3324 (NH_2), 1689 (C=O), ^{1}H-NMR (DMSO-d6) (δ ppm): 4.50 (s, 1H, pyran-CH), 7.20 (m, 2H, Ar-H), 7.28 (m, 3H, Ar-H), 7.35 (m, 5H, Ar-H),7.45 (m, 2H, Ar-H), 7.79-7.81 (m, 2H, Ar-H), 8.20 (s, 1H, CH), 8.63 (s, 2H, NH_2 exchangeable), Analysis Calcd. For $C_{26}H_{18}ClN_5O$

(451.91) C, 69.10; H, 4.01; N, 15.50; Found: C, 69.20; H, 4.08; N, 15.40

5-amino-4-(2-chlorophenyl)-1,3-diphenyl-4,8-dihydropyrazolo[4',3':5,6]pyrano [2,3-d]pyrimidine-7(1H)-thione (8)

A mixture of **4** (2.12g, 5 mmol) and thiourea (5 mmol) in toluene was refluxed on a hot plate for 24 hours. the excess solvent was removed under vacuum; the solid remains was crystallized from ethanol to give **8** as dark brown crystal; yield; 94%; m.p.117-119℃; ^{1}H-NMR (DMSO-d_6) (δ ppm): 4.50 (s, 1H, pyran-CH), 7.20 (m, 2H, Ar-H), 7.28 (m, 3H, Ar-H), 7.35 (m, 5H, Ar-H),7.45 (m, 2H, Ar-H), 7.79-7.81 (m, 2H, Ar-H), 8.63 (s, 2H, NH_2 exchangeable), 9.84 (s, 1H, NH exchangeable), ^{13}C-NMR (DMSO-d_6) (ppm): 30, 69 (2CH), 120- 155 (Ar-C), 162 (C-NH_2), 184 (C=S) ; Analysis Calcd. For $C_{26}H_{18}ClN_5OS$ (483.97) C, 64.52; H, 3.75; N, 14.47; Found: C, 64.45; H, 3.65; N, 14.40.

5-amino-4-(2-chlorophenyl)-1,3-diphenyl-4,8-dihydropyrazolo[4',3':5,6] pyrano[2,3-d]pyrimidine-7(1H)-one (9)

A mixture of **4** (2.12g, 5mmol) and urea (0.3 g, 5mmol) in toluene (20 mL) was refluxed for 24 hours. the excess solvent was removed under vacuum; the solid remained was crystallized from methanol to give **9** as dark brown crystal; yield; 90%; IR (KBr): ύ /cm^{-1}: 3324 (NH_2), 1689 (C=O), ^{1}H-NMR (DMSO-d_6) (δ ppm): 4.50 (s, 1H, pyran-CH), 7.20 (m, 2H, Ar-H), 7.28 (m, 3H, Ar-H), 7.35 (m, 5H, Ar-H),7.45 (m, 2H, Ar-H), 7.79-7.81 (m, 2H, Ar-H), 8.04 (s, 2H, NH_2 exchangeable), 9.84 (s, 1H, NH exchangeable), m.p.110-112℃; Analysis Calcd. For $C_{26}H_{18}ClN_5O_2$ (467.91) C, 66.74; H, 3.88; N, 14.97; Found: C, 66.71; H, 3.80; N, 14
.99.

6-amino-4-(2-chlorophenyl)-1,3-diphenyl-1,4-dihydropyrano[2,3-c] pyrazole-5-carboxamid (10)

Compound **4** (2.12g, 5 mmol) was added dropwise with stirring to conc. cold sulfuric acid (6 mL) at 20℃, the temperature does not exceed 40℃ then the solution was stirred for further an hour at room temperature and poured onto an ice cold water (10 mL).the reaction mixture was left overnight in the refrigerator. The precipitate was filtered off and recrystallized from chloroform to give **10** as brown crystal; yield; 95%; m.p.97-99℃; IR (KBr): ύ /cm^{-1}: 3390 (NH_2), 1660 cm^{-1} (CO);), ^{1}H-NMR (DMSO-d_6) (δ ppm): 4.50 (s, 1H, pyran-CH), 6.0, 7.0 (2s, 4H, 2NH_2 exchangeable), 7.20 (m, 2H, Ar-H), 7.28 (m, 3H, Ar-H), 7.35 (m, 5H, Ar-H),7.45 (m, 2H, Ar-H), 7.79-7.81 (m, 2H, Ar-H), Analysis Calcd. For $C_{25}H_{19}ClN_4O_2$ (442.90) C, 67.80; H, 4.32; N, 12.65; Found: C, 67.75; H, 4.21; N, 12.70.

4-(2-Chloro-phenyl)-6-(2-(D-Glucopentitolylideneamino)-1,3-diphenyl-1,4-dihydro-pyrano[2,3-c]pyrazole-5-carbonitrile (11)

A solution of **4** (4.2g, 0.01mol) and *D*-glucose (1.8g, 0.01mol) in absolute ethanol (20 mL) containing few drops of glacial acetic acid was refluxed for 7-10 h. The formed solid, after cooling was filtered, washed with water, air dried and crystallized from ethyl acetate to give **11** as dark brown crystals; yield; 64% ; m.p.143-145℃; IR (KBr): ύ /cm^{-1}: 3322-3198 (OH) cm^{-1}; ^{1}H-NMR (DMSO-d_6) (δ ppm): 3.42–3.55 (m, 2H, H-6`,6``), 3.82-3.90 (m, 2H, H-5`, OH), 4.32-4.39 (m, 3H, H-4`, H-3`, OH), 4.50 (s, 1H, pyran-CH), 4.58 (m, 1H, OH), 4.72-4.88 (m, 3H, H-2`, 2OH), 7.20 (m, 2H, Ar-H), 7.28 (m, 3H, Ar-H), 7.35 (m, 5H, Ar-H),7.45 (m, 2H, Ar-H), 7.79-7.81 (m, 2H, Ar-H), 8.7 (s, 1H, N=CH); Analysis Calcd. For $C_{31}H_{27}ClN_4O_6$ (587.02) C, 63.43; H, 4.64; N, 9.54; Found: C, 63.40; H, 4.60; N, 9.50.

4-(2-Chloro-phenyl)-6-[(4-methoxy-benzylidene)-amino]-1,3-diphenyl-1,4-dihydro-pyrano[2,3-c]pyrazole-5-carbonitrile (12)

To a solution of **4** (4.2g,0.01mol) and *p*-methoxy benzaldehyde (1.2 ml, 0.01mol) in absolute ethanol (20 mL) containing few drops of glacial acetic acid was refluxed for 7-10 h. the formed solid, after cooling was filtered, washed with water, air dried and crystallized from benzene to give **12** as light brown crystals; yield; 52%; m.p.103-105℃; IR (KBr): ύ /cm^{-1}: 3060 (CH), 2202 (CN) cm^{-1}; ^{1}H-NMR (DMSO-d_6) (δ ppm): 4.11 (s, 3H, OCH_3), 4.50 (s, 1H, pyran-CH), 6.9 (d, 2H, Ar-H), 7.20 (m, 2H, Ar-H), 7.28 (m, 3H, Ar-H), 7.35 (m, 5H, Ar-H),7.45 (m, 2H, Ar-H), 7.79-7.81 (m, 2H, Ar-H), 8.0 (d, 2H, Ar-H), 9.5 (s, 1H, N=CH); ^{13}C-NMR (DMSO-d6) (δ ppm): 23, 56 (2CH), 85 (C-CN), 115-132, 150-154 (Ar-C), 164 (CH=N), 168 (=CH-O); Analysis Calcd. For $C_{33}H_{23}ClN_4O_2$ (543.01) C, 72.99; H, 4.27; N, 10.32; Found: C, 72.90; H, 4.21; N, 10.29.

4-(2-Chloro-phenyl)-6-[(4-dimethylamino-benzylidene)-amino]-1,3-diphenyl-1,4-dihydro-pyrano[2,3-c]pyrazole-5-carbonitrile (13)

A solution of **4** (4.2g, 0.01 mol) and 4-dimethyl amino benzaldehyde (1.4g, 0.01mol) in absolute ethanol (20 mL) containing few drops of glacial acetic acid was refluxed for 7-10 h. the formed solid, after cooling was filtered, washed with water, air dried and crystallized from ethanol to give **13** as reddish brown color; yield; 88%; m.p.87-90℃; ^{1}H-NMR (DMSO-d_6) (δ ppm): 3.0, 3.09 (2s, 6H, 2CH_3), 4.50 (s, 1H, pyran-CH), 6.9 (d, 2H, Ar-H), 7.20 (m, 2H, Ar-H), 7.28 (m, 3H, Ar-H), 7.35 (m, 5H, Ar-H),7.45 (m, 2H, Ar-H), 7.79-7.81 (m, 2H, Ar-H), 8.0 (d, 2H, Ar-H), 9.5 (s, 1H, N=CH); Analysis Calcd. For $C_{34}H_{26}ClN_5O$ (556.06) C, 73.44; H, 4.71; N, 12.59; Found: C, 73.40; H, 4.67; N, 12.70.

4-(2-chlorophenyl)-1,3,7-triphenyl-1,4-dihydro-5H-pyrazolo[4',3':5,6]- pyrano[2,3-d][1,3]oxazin-5-one (14)

A mixture of **4** (2.1g, 5 mmol) and benzoyl chloride (0.7g, 5 mmol) in toluene was refluxed for 24 hours. the excess solvent was removed under vacuum; the solid remained was crystallized from petroleum ether to give **14** as brown crystals; yield; 80%; m.p.78-80℃; ^{1}H-NMR (DMSO-d6) (δ ppm): 4.50 (s, 1H, pyran-CH), 7.20 (m, 2H, Ar-H), 7.28 (m, 3H, Ar-H), 7.35 (m, 5H, Ar-H),7.45 (m, 2H, Ar-H), 7.46 (m, 2H, Ar-H), 7.79-7.81 (m, 2H, Ar-H), 7.92 (m, 3H, Ar-H), 3H, Ar-H), ^{13}C-NMR (DMSO-d6) (δ ppm): 24, 65 (2CH), 85 (=CH), 128-152 (Ar-C), 172 (C=O); Analysis Calcd. For $C_{32}H_{20}ClN_3O_3$ (529.97) C, 72.52; H, 3.80; N, 7.93; Found: C, 72.50; H, 3.75; N, 7.95.

N-[4-(2-Chloro-phenyl)-5-cyano-1,3-diphenyl-1,4-dihydro-pyrano[2,3-c] pyrazol-6-yl]-formimidic acid ethyl ester (15)

A mixture of compound **4** (4.2g, 0.01mol) and triethyl orthoformate (0.37 g, 0.01mol) in the presence of acetic anhydride (20 mL) was refluxed for 6 h, cooled at room temperature. the resulting solid was filtered and recrystallized by benzene to afford compound **15** as brown crystals; yield; 60%; m.p.141-143℃; IR (KBr): ύ /cm^{-1}: 3160 (NH), 2194 (CN) cm^{-1}; ^{1}H-NMR (DMSO-d_6) (δ ppm): 1.90 (t, 3H, CH_3), 3.9 (q, 2H, CH_2), 4.50 (s, 1H, pyran-CH), 7.20 (m, 2H, Ar-H), 7.28 (m, 3H, Ar-H), 7.35 (m, 5H, Ar-H),7.45 (m, 2H, Ar-H), 7.79-7.81 (m, 2H, Ar-H), 9.50 (s,1H, N=CH); ^{13}C-NMR (DMSO-d6) (ppm): 15 (CH_3), 24, 65 (2CH), 63 (CH_2), 85 (=CH), 128-152 (Ar-C), 168 (=CH-O); Analysis Calcd. For $C_{28}H_{21}ClN_4O_2$ (480.94) C, 69.92; H, 4.40; N,11.65; Found: C, 69.90; H, 4.41; N, 11.70.

4-(2-chlorophenyl)-5-imino-1,3-diphenyl-1,4-dihydropyrazolo[4',3':5,6] pyrano[2,3-d]pyrimidin-6(5H)-amine (16)

A solution of compound **15** (4.8g, 0.01mol) with of hydrazine hydrate (0.5g, 0.01mol) in the presence of absolute ethanol (20 mL) was refluxed for 6 h, cooled at the room temperature. the resulting solid was recrystallized by benzene to afford compound **16** as brown crystals; yield;97%; m.p.121-123℃; IR (KBr): ύ /cm^{-1}: 3395-3210 (NH_2 and NH) cm^{-1}; ^{1}H-NMR (DMSO-d_6) (δ ppm): 4.50 (s, 1H, pyran-CH), 5.99 (s, 2H, NH_2 exchangeable), 7.20 (m, 2H, Ar-H), 7.28 (m, 3H, Ar-H), 7.35 (m, 5H, Ar-H),7.45 (m, 2H, Ar-H), 7.79-7.81 (m, 2H, Ar-H), 9.0 (s, 1H, pyrimidine CH); 9.69 (s, 1H, NH exchangeable), Analysis Calcd. For $C_{26}H_{19}ClN_6O$ (466.92) C, 66.88; H, 4.10; N, 18.00; Found: C, 66.90; H, 4.21; N, 17.98.

5-((4-(2-chlorophenyl)-5-imino-(6(5H)-2-(D-xylotetritolylideneamino))-1,3-diphenyl-1,4-dihydro pyrazolo[4',3':5,6]pyrano[2,3-d]pyrimidine (17)

Reaction of compound **16** with *D*-Xylose (4.6g, 0.01mol) in the presence of ethanol (20 mL) and catalytic compound of glacial acetic acid (1ml) was stirred for 30 min then refluxed for 3h, cooled at the room temperature. the resulting solid was recrystallized by xylene to afford compound **17** as brown crystals; yield; 84%; m.p.138-140℃; IR (KBr): ύ /cm^{-1}: 3557-3193 (OH and NH) cm^{-1}; ^{1}H-NMR (DMSO-d_6) (δ ppm): 3.82-3.90 (m, 2H, H-5`, 5``), 4.32-4.39 (m, 3H, H-4`, H-3`, OH), 4.50 (s, 1H, pyran-CH), 4.58 (m, 1H, OH), 4.72-4.88 (m, 3H, H-2`, 2OH), 7.20 (m, 2H, Ar-H), 7.28 (m, 3H, Ar-H), 7.35 (m, 5H, Ar-H),7.45 (m, 2H, Ar-H), 7.79-7.81 (m, 2H, Ar-H), 7.90 (s, 1H, N=CH); 9.0 (s, 1H, pyrimidine CH); 9.69 (s, 1H, NH exchangeable), ^{13}C-NMR (DMSO-d6) (δ ppm): 21, 56, 70, 85, 95 (5 CH), 122-139 (Ar-C), 149 (N=CH), 160 (C=NH); Analysis Calcd. For $C_{31}H_{27}ClN_6O_5$ (599.04) C, 62.16; H, 4.54; N, 14.03; Found: C, 62.20; H, 4.50; N, 14.10.

10-(2-chlorophenyl)-7,9-diphenyl-7,10-dihydro-2H-[1,3]diazeto[1,2-c] pyrazolo[4',3':5,6]pyrano[3,2-e]pyrimidine-2-thione (18)

A mixture of compound 16 (4.6g, 0.01mol) and CS_2 (2 mL) in the presence of KOH (0.56 g) and ethanol (20 mL) was stirred for one hour then refluxed for 6h, cooled at room temperature. The resulting solid was recrystallized by ethanol to afford compound **18** as brown crystal; yield; 89%; m.p.178-180℃; ^{1}H-NMR (DMSO-d_6) (δ ppm): 4.50 (s, 1H, pyran-CH), 7.20 (m, 2H, Ar-H), 7.28 (m, 3H, Ar-H), 7.35 (m, 5H, Ar-H),7.45 (m, 2H, Ar-H), 7.79-7.81 (m, 2H, Ar-H), 9.0 (s, 1H, pyrimidine CH); Analysis Calcd. For $C_{27}H_{16}ClN_5OS$ (493.97) C, 65.65; H, 3.26; N, 14.18; Found: C, 65.70; H, 3.21; N, 14.20.

Biological assessment

1. Antimicrobial assay

Experimental

Bacillus cereus B-3711 and *Asperagillus flavus* 3357 were provided by the Northern Regional Research Laboratory Illinois, USA (NRRL). *Listeria monocytogenes* 598 was provided by the Department of Food Science, University of Massachusetts, USA. *Escherichia coli* 0157:H7, *Salmonella typhmirum* and *Staphylococcus aureus* were isolated from serologically identified by Dairy microbiological Lab., National Research Center. *Yersinia enterocolitica* was obtained from Hungarian National Collection of Medical Bacteria, OKI, Gyaliut 2-6, H-1966 Budapest, Hungary.

The stock solutions of the compounds under study (**3-18**) were prepared at conc. (1 mg/ml) for antibacterial and antifungal assay. Sterile discs were impregnated with 10 µL of each for anti-bacterial and antifungal

assay 10 µg /disk) a loading control was also prepared containing 10 µL of Dimethyl sulfoxide (DMSO) for each inoculated spread plate. The discs of (**3-18**) were placed on the surface of the agar plat using sterile forceps, gently press down each disc to ensure complete contact with the agar surface. Antimicrobial activity of the selected compounds (**3-18**) was conducted against a wide range of human pathogenic microorganisms Gram positive bacteria (*S. aureus*, *B. cereus* and *L. monocytogenes*), Gram negative bacteria (*Y. enterocolitica*, *S. typhmirum* and *E. coli*) and fungal strain (*Fusarium sp.* and *Aspergillus niger*). Cefoperazone and Clotrimazole were used as positive controls for bacteria and fungi, respectively at 100 at conc. (100 µg/ml), while DMSO solution (10% v/v) was used as a negative control. The inverted plates were incubated at (37°C -18 h) for bacteria and (25°C -3 days) for fungi after the discs are applied. The diameter of inhibition zones was measured to the nearest whole millimeter, including the diameter of the disc, using sliding calipers, which is held on the back of the inverted Petri plate. Plates were examined for growth inhibition and the diameter of the inhibition zone measured. Plates were examined at the end of incubation period and the zone of inhibition (ZOI) of diameter was noted as mean values (n=3) and was expressed in (cm). The strength of the activity was classified as high activity for the inhibition zone having diameters of (10-15 mm) and low activity for the diameter ranging from (7-10 mm) and no activity for one with diameter less than 7 mm. All the data were calculated in mean ± SD pattern by performing in triplicates.

2. The DPPH assay for evaluation of antioxidant activity

In vitro the antioxidant activity was evaluated by 2.2-diphenyl-1-picrylhydrazyl free radical scavenging assay according to the method of [36]**.** Briefly, 100 µl of each concentration (300, 150, 75, 37.5 µg/ml) were taken in different test tubes was added to 1 mL of 0.1 mM ethanol solution of DPPH and shaken vigorously. The tubes were then incubated at 37 C^0 for 30 min. Changes in the absorbance were measured at 517 nm against a blank, i.e. without DPPH using UV-Vis Shimadzu (UV-1601, PC) spectrophotometer. Ethanol was used to zero spectrophotometer. Measurement was performed in triplicate and an average was used. The radical scavenging activity was expressed as percentage inhibition of DPPH using the following formula:

% Inhibition = $[(A_{control} - A_{treatment}/A_{control})]$ X 100

Where: $A_{control}$: is the absorbance of the control; $A_{treatment}$: is the absorbance of the treatments. Ascorbic acid was used as positive controls.

3. Cytotoxicity assay

MTT assay for Cell Viability and Proliferation

This assay was carried out according to the method described by [37]. In this assay, the promising compounds were used to determine the inhibitory effects on cell growth. This colorimetric assay is based on the conversion of the yellow tetrazolium bromide (MTT) to a purple formazan derivative by mitochondrial succinate dehydrogenase in viable MCF-7 cell lines. Cell lines were cultured in RPMI-1640 medium (Sigma Co. St. Louis, USA) with 10% fetal bovine serum (GIBCO, UK). Antibiotics (100 units/ml penicillin and 100 µg/ml streptomycin) were added to the media and incubated at 37 ºC in a 5% Co2 incubator. Then the cell lines were seeded in a 96-well plate at a density of $1.0x10^4$ cells/well at 37 ºC for 48 h under 5% Co_2. After the incubation period, the cells were treated with different concentrations of the synthesized compounds and incubated for 24 h. After 24 h of the treatment, 20 µl of MTT (Sigma, St., USA) solution at 5 mg/ml was added and incubated for 4 h. Dimethyl sulfoxide (DMSO; Sigma, St., USA) in volume of 100 µl was added into each well to dissolve the purple formazan formed. The colorimetric assay was measured and recorded at absorbance of 570 nm using a plate reader (EXL 800, USA), Doxorubicin was used as a standard anticancer drug for comparison.

The relative cell viability in percentage was calculated as follow:

(A570 of treated samples/A570 of untreated sample) X 100

Molecular docking (MD) simulation

The molecular docking of the new synthesized compounds **(4**, **8, 17** and **18**) with the VEGFR-2 protein (PDB code: 4ASD) in association with an inhibitor sorafenib (PDB ID: 4ASD) was performed using 2019.01 (Molecular Operating Environment, Version 2019.01, Chemical Computing Group Inc., Montreal, Canada). The crystal structure of VEGFR-2 protein was retrieved from the protein data bank at http://www.rscb.org./pdb using 4ASD codes[40] .The water molecules were removed and the enzyme was prepared using *QuickPrep* tool module in MOE 2019.01 then the active site was identified. The co-crystallized ligand was re-docked into the enzyme active pocket to validate our docking protocol.

The chemical structure of the selected molecules was constructed with the *ChemDraw* ultra 10.0 and saved as mol file and loaded into to MOE program. All structures were protonated and minimized using the MMFF94x force field until the RMSD of 0.01 Å was reached. The induced-fit protocol was used in the docking simulation, with the Triangle Matcher method used to place ligand conformations in the site, which were then ranked using the London ΔG scoring

function. For each compound, one hundred docking poses were calculated, and the resulting docking poses were visualized using MOE 2019.01. The top-scored docking poses were used to calculate the binding free energy (ΔG) of compounds and co-crystallized ligand in kcal/mol.

3. Results

Chemistry

Claisen-Schmidt condensation reaction between 2,5-Diphenyl-2,4-dihydro-pyrazol-3-one **(1)** with 2-chlorobenzaldehyde **(2)** in ethanol / sodium hydroxide solution afforded the chalcone derivative **3**. The structure of compound **3** was elucidated by IR and ^{1}H NMR spectroscopic data where IR spectrum of **3** shows aromatic HC=CH and C=O at 3061 and 1712 Cm^{-1} respectively. While ^{1}H NMR spectrum reveals signals of the aromatic protons at 7.20-7.79 ppm in addition to a signal at 7.81 ppm for C=CH proton.

Reaction of compound **3** with malononitrile in absolute ethanol and few drops of piperidine gave 6-amino-4-(2-chlorophenyl)-1,3-diphenyl-1,4-dihydropyrano[2,3-c] pyrazole-5-carbonitrile **4** in a good yield. The structure of compound **4** was elucidated by IR and ^{1}H NMR spectroscopic data where, IR spectrum shows strong vibration bands at 3310 and 2188 Cm^{-1} for NH_2 and CN respectively. While, ^{1}H NMR spectrum reveals signals of the aromatic protons at δ 7.28-7.44 ppm in addition to a singlet signal at δ 6.81 ppm for NH_2 protons (D_2O exchangeable).

Furthermore, compound **4** was used as a key starting material for synthesizing and Designing of a series of new heterocyclic compounds with potent biological activities. So, reaction of compound **4** with formic acid upon reflux temperature afforded 4-(2-chlorophenyl)-1,3-diphenyl-4,6,7,8-tetrahydropyrazolo[4',3':5,6]pyrano[2,3-d]pyrimidin-5(1H)-one **5**.

The structure of compound **5** was confirmed by IR and ^{1}H NMR spectroscopic data where IR spectrum inferred strong vibration bands at 3193 and 3163 Cm^{-1} for two NH groups respectively. ^{1}H NMR spectrum reveals signals of the aromatic protons at δ 7.33-7.63 ppm in addition to signals at δ 8.3 and 1.3 ppm for 2 NH groups and at δ 5.8 ppm assigned for CH_2 group of the pyrimidine moiety. Also, ^{13}C NMR spectrum gives another proof for the structure of compound **5** which showed signals at δ 170 for C=O group. [*c.f.* Experimental part]

Boiling of **4** with acetic anhydride under reflux afforded 4-(2-chlorophenyl)-7-methyl-1,3-diphenyl-1,4-dihydro-5H-pyrazolo[4',3':5,6]pyrano[2,3-d][1,3]oxazin-5-one **6**. Which its structure confirmed by IR and ^{1}H NMR spectroscopic data where IR spectrum of **6** shows strong vibration bands at 3063 cm^{-1} for aromatic CH group. ^{1}H NMR spectrum of **6** reveals signals of the aromatic protons at δ 7.10-7.81 ppm in addition to a signal at 1.0 ppm for methyl group of the oxazinone ring moiety. Also, reaction of **4** with formamide under reflux and stirring gave 4-(2-chlorophenyl)-1,3-diphenyl-1,4-dihydropyrazolo[4',3':5,6]pyrano[2,3-d]pyrimidin-5-amine **7** in a good yield.

The structure of compound **7** was confirmed by IR and ^{1}H NMR spectroscopic data where IR spectrum of **7** inferred strong vibration bands at 3423 Cm^{-1} for two NH_2 group of the pyrimidine moiety. ^{1}H NMR spectrum of **7** reveals signals of the aromatic protons at δ 7.0 – 7.99 ppm in addition to two singlet signals at 8.64 and 5.99 ppm for pyrimidine CH and NH_2 (D_2O exchangeable) groups respectively.

Boiling of compound **4** with thiourea in toluene under reflux afforded 5-amino-4-(2-chlorophenyl)-1,3-diphenyl-4,8-dihydropyrazolo[4',3':5,6]pyrano[2,3-d]pyrimidine-7(1H)-thione **8** in a good yield.

The structure of compound **8** was assigned by ^{1}H NMR and ^{13}C NMR spectroscopic data where ^{1}H NMR spectrum of **8** shows signals of the aromatic protons in addition to signals at δ 9.84 and 8.63 ppm for thiopyrimidine NH and NH_2 (D_2O exchangeable) groups respectively. Also, ^{13}C NMR gives another proof for the structure of compound **8**. [Experimental part].

While, Boiling of **4** with urea in toluene under reflux afforded 5-amino-4-(2-chlorophenyl)-1,3-diphenyl-4,8-dihydropyrazolo[4',3':5,6]pyrano[2,3-d]pyrimidine-7(1H)-one **9** in a good yield.

The structure of compound **9** was deduced by IR and ^{1}H NMR spectroscopic data where IR spectrum of **9** referrers strong vibration bands at 3390 and 3160 cm^{-1} for NH_2 and NH groups respectively. ^{1}H NMR spectrum of **9** shows signals of the aromatic protons in addition to signals at δ 9.84 and 8.04 ppm for Oxa-pyrimidine NH and NH_2 (D_2O exchangeable) groups respectively. [Scheme 1 & Experimental Section]

Stirring of **4** with conc. Cold H_2SO_4 afforded 6-Amino-4-(2-chloro-phenyl)-1,3-diphenyl-1,4-dihydro-pyrano[2,3-c]pyrazole-5-carboxylic acid Amide **10** in a good yield .

The structure of compound **10** was assigned by IR and ^{1}H NMR spectroscopic data where the IR spectrum of **10** referrers strong vibration bands at 3390 and 1160 Cm^{-1} for NH_2 and CO groups respectively. ^{1}H NMR spectrum of 10 shows signals of the aromatic protons in addition to signals at δ 7.0 and 6.0 ppm for two NH_2 (D_2O exchangeable) groups respectively.

Reaction of compound **4** with D-glucose in absolute ethanol and few drops of glacial acetic acid gave 4-(2-Chloro-phenyl)-6-(2,3,4,5,6-pentahydroxy-

hexylideneamino)-1,3-diphenyl-1,4-dihydro-pyrano[2,3-c]pyrazole-5-carbonitrile **11**.

The structure of compound **11** was assigned by IR and ^{1}H NMR spectroscopic data where IR spectrum of **11** referrers strong vibration bands at 3500-3450 and 2210 Cm^{-1} for sugar OH and CN groups respectively. ^{1}H NMR spectrum of 10 shows signals of the aromatic protons in addition to signals at δ 8.7 and 3.59-5.4 ppm for N=CH and the sugar protons.

Condensation of Compound **4** with *p*-methoxybenzaldehyde in absolute ethanol containing few drops of glacial acetic acid gave 4-(2-Chloro-phenyl)-6-[(4-methoxy-benzylidene)-amino]-1,3-diphenyl-1,4-dihydro-pyrano[2,3-c]pyrazole-5-carbonitrile **12**. Its structure was deduced by IR and ^{1}H NMR spectroscopic data where IR spectrum of **12** referrers strong vibration bands at 2200 Cm^{-1} for CN group. ^{1}H NMR spectrum of **12** shows signals of the aromatic protons in addition to signals at δ 9.49 and 4.11 ppm for N=CH and OCH_3 groups respectively. Also, ^{13}C NMR gives another proof for the structure of compounds **12** which inferred signals at δ 164 and 168 ppm for CH=N and =CH-O groups respectively.

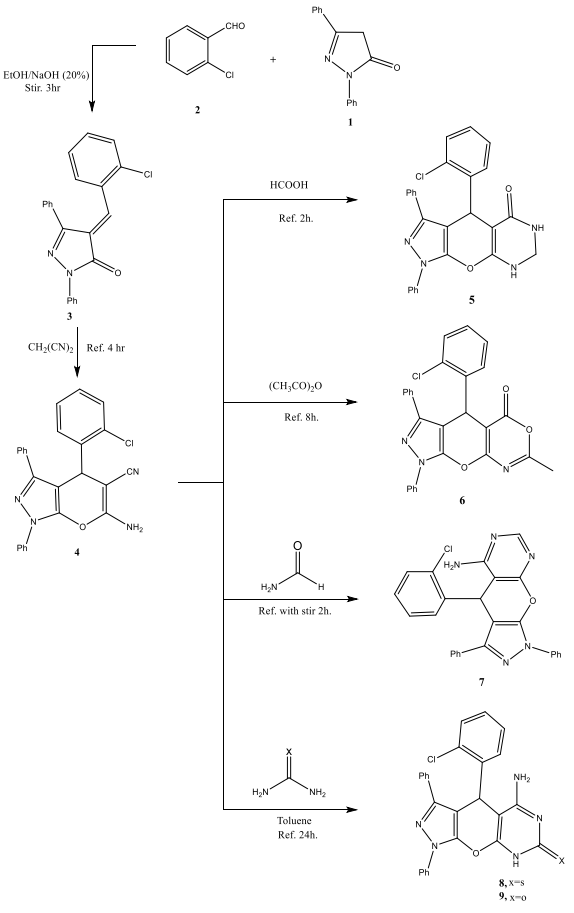

Scheme 1; Synthesis of compounds 3-9

Also, condensation of compound 4 with 4-dimethyl amino benzaldehyde in absolute ethanol containing few drops of glacial acetic acid gave 4-(2-Chloro-phenyl)-6-[(4-dimethylamino-benzylidene)-amino]-1,3-diphenyl-1,4-dihydro-pyrano[2,3-c] pyrazole-5-carbonitrile **13** in a good yield.

The structure of compound **13** was assigned by IR and ^{1}H NMR spectroscopic data where IR spectrum referrers strong vibration bands at 2200 Cm^{-1} for CN group. ^{1}H NMR spectrum of **12** shows signals of the aromatic protons in addition to signals at δ 9.60 and 3.0 and 3.09 ppm for N=CH and $N(CH_3)_2$ groups respectively.

Benzoylation of compound **4** with benzoyl chloride afforded 4-(2-chlorophenyl)-1,3,7-triphenyl-1,4-dihydro-5H-pyrazolo[4',3':5,6]pyrano[2,3-d][1,3]oxazin-5-one **14**.

The structure of compound **14** was determined by IR and ^{1}H NMR spectroscopic data where IR spectrum inferred strong vibration bands at 3000 cm^{-1} for CH group. ^{1}H NMR spectrum shows signals of the aromatic protons at δ 7.24- 7.92 ppm. Also, ^{13}C NMR gives another proof for the structure of compounds **14** which inferred signals at δ 172 ppm for C=O group. [Scheme 2 & Experimental Section]

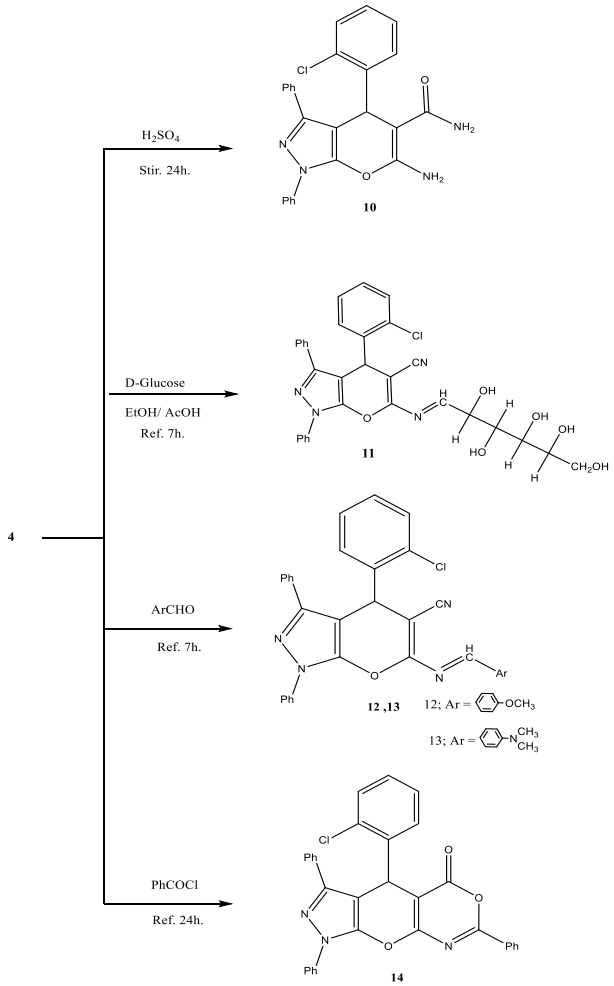

Scheme 2. Synthesis of compounds 10-14

On the other hand, reaction of compound **4** with triethyl orthoformate in the presence of acetic anhydride upon reflux temperature afforded N-[4-(2-Chloro-phenyl)-5-cyano-1,3-diphenyl-1,4-dihydro-pyrano[2,3-c]pyrazol-6-yl]-formimidic acid ethyl ester **15** in a good yield.

The structure of compound **15** was obtained by IR and ^{1}H NMR spectroscopic data. IR spectrum shows strong vibration bands at 3060, 2929, 2155 Cm^{-1} for CH, and CN groups respectively. ^{1}H NMR spectrum of **15** shows signals of the aromatic protons at δ 7.28-7.91 ppm in addition to singlet, triplet and quartet signals at δ 9.55, 1.88 and 3.93 ppm for N=CH, CH_3 and CH_2 groups respectively. Also, ^{13}C NMR gives another proof for the structure with signals at δ 168 ppm for (=CH-O). [Scheme 3 & Experimental Section]

Compound **15** then reacted with hydrazine hydrate in absolute ethanol to afford 4-(2-chlorophenyl)-5-imino-1,3-diphenyl-1,4-dihydropyrazolo[4',3':5,6]pyrano[2,3-d]pyrimidin-6(5H)-amine **16**. The structure of compound **16** was infrared by IR and ^{1}H NMR spectroscopic data. IR spectrum shows strong vibration bands at 3477, 3210 cm^{-1} for NH_2 and NH groups respectively. ^{1}H NMR spectrum inferred signals of the aromatic protons at δ 7.28- 7.91 ppm in addition to three singlet signals at δ 9.69, 9.00 and 5.99 ppm for NH, N=CH and NH_2 groups respectively. [Scheme 3& Experimental Section.]

Stirring of compound **16** with D-xylose in the presence of ethanol and catalytic compound of glacial acetic acid for 30 minutes then reflux afforded the amino sugar derivative **17** in a good yield.

The structure of compound **17** was deduced by IR and ^{1}H NMR spectroscopic data. IR spectrum of **17** shows strong vibration bands at 3537-3193 Cm^{-1} for sugar OH and NH groups respectively. ^{1}H NMR spectrum of **17** shows signals of the aromatic protons at δ 7.28- 7.91 ppm in addition to three singlet signals at δ 9.67, 7.90 and 3.30-5.90 ppm for NH, N=CH and sugar protons groups respectively. Also, ^{13}C NMR gives another proof for the structure of compounds **17** with signals at δ 149 and 160 ppm for (N=CH) and (C=NH) groups respectively.

Stirring of compound **16** with CS_2 in the presence of KOH for one hour then reflux afforded 10-(2-chlorophenyl)-7,9-diphenyl-7,10-dihydro-2H-[1,3]diazeto[1,2-c] pyrazolo[4',3':5,6]pyrano[3,2-e]pyrimidine-2-thione **18** in a good yield.

The structure of compound **18** was deduced by IR and ^{1}H NMR spectroscopic data. IR spectrum shows strong vibration bands at 3090 cm^{-1} for CH groups respectively. ^{1}H NMR spectrum inferred signals of the aromatic protons at δ 7.28- 7.91 ppm in addition to a singlet signal at δ 8.18 ppm for N=CH group. [Scheme 3 & Experimental section]

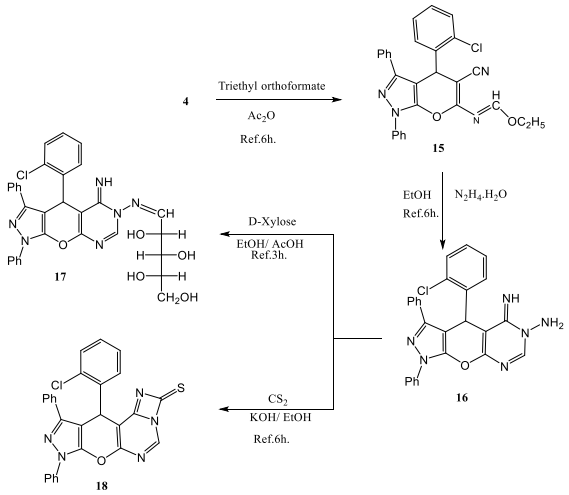

Scheme 3; Synthesis of Compounds 15-18

Antimicrobial assay

***In vitro*, assessment of antibacterial activity of tested compounds (3-18) against some of pathogenic bacteria**

The present study was conducted to determine the antimicrobial potential of the synthesized compounds (**3-18**) against the pathogenic bacteria using Disc inhibition assay. Table (1) shows the mean of the diameter of zone of inhibition for each compound. The sensitivity of the bacterial pathogens to the tested compounds was compared with cefoperazone as a standard drug to reveal the efficacy of synthesized compounds.

The results of antimicrobial activity screening revealed that the synthesized compounds showed antibacterial activity that varied among the tested microbial strains.

Herein, we highlight on the compound **18** that exhibited promising antibacterial activity against *L. monocytogenes* and *S. typhmirum* (17.5, 17 mm, respectively) and was higher than that of cefoperazone, which was used as a reference drug (16 mm). Moreover, its antibacterial activity was highly active against other tested Gram-negative bacteria *E. coli* (15.5 mm) and *Y. enterocolitica* (14 mm). On the other hand, compound **8** showed a potent activity against *Y. enterocolitica* strain (18.5 mm) comparing to cefoperazone (15.5 mm). Also compounds **(3, 5, 9, 11, 13, 14** and **18)** displayed satisfactory activities against *Y. enterocolitica* range between (9.5-15.5 mm). However, an entirely different trend in antibacterial activity against *Y. enterocolitica* was observed with compounds **(6, 15, 16)** that were inactive against it, also against *S. typhmirum* for compounds **(10, 12, 13, 17)**. The findings of the current study showed that there were differences between the antimicrobial activities between the tested compounds due to the tested bacteria differ in

their cell wall and, their susceptibility to antimicrobial agents. It is a well-known fact that the outer layer in Gram-positive bacteria (peptidoglycan layer) does not offer effective barrier against antimicrobial agents compared to the out layer found in Gram-negative organisms (phospholipid membrane containing lipopolysaccharide).So, It is possible that for some compounds (**6, 10, 12, 13, 15** and **16**) the lack of Gram-negative activity in *Y. enterocolitica* and *S. typhmirum* is due to limited cellular entry or susceptibility to extensive efflux pump removal from the bacteria, and additional structural modifications might be able to overcome these barriers. There is a dire need for new antimicrobial compounds to combat the growing threat of widespread antibiotic resistance, so it is important to raise awareness of these types of compounds for the design of truly novel antibiotics with potential for combatting antimicrobial resistance.

In vitro, assessment of antifungal activity of tested compounds (3-18) against some of pathogenic fungi

In vitro Antifungal activity was screened for the newly synthesized compounds (**3-18**) by agar diffusion method using two fungal strains *Fusarium sp*. and *Aspergillus niger*. Compound **8** displayed excellent antifungal activity against *Fusarium sp* with an inhibition zone 30.5 mm comparing with the standard. While, the compounds (**3, 4, 5, 6, 7, 11, 14, 15** and **16**) are inactive and the others were moderate to less active.

The variation in the efficiency of different compounds against microorganism depends on either the cell impermeability of the microbes or on differences in the ribosomes of the microbial cell [34]. It is obvious that compound **8** exhibited a potent inhibition activity against *Fusarium sp* and showed remarkable fungicidal activities owing to its characteristic skeleton that containing substituent naphthalene-2-thione

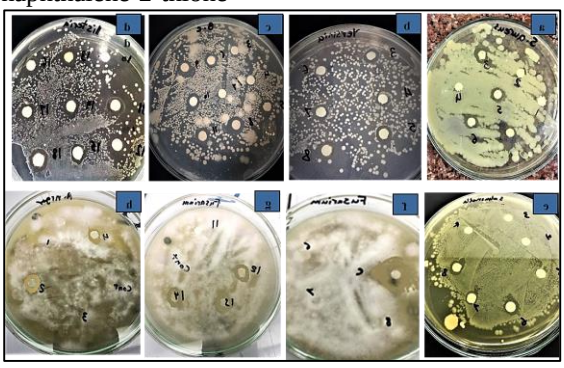

Figure (1). The effect of synthesized compounds on the growth of pathogenic bacteria and fungi by disc diffusion assay.

a. S. aureus,
b. Y. enterocolitica
c. B. cerus
d. . L. monocytogenes
e. S. typhi
f. Fusarium sp
g. Fusarium sp
h. *A. niger*

The DPPH assay for evaluation of antioxidant activity

The antioxidant activity of the compounds was investigated using DPPH that is well known used for measuring the antioxidant power of various compounds. During the DPPH free radical reaction, the decrease in absorbance, which led to the discoloration of the DPPH solution, indicates the scavenging potential of each compound. The bioactive compounds present in this study can discolor DPPH solution by their hydrogen- donating ability. In (Figure 2), the lowest antioxidant activity was observed in compounds (**13** and **12**) at conc. 30 µg/ml while compound **8** recorded the highest scavenging. The increasing scavenging activity upon increasing concentration of the compounds **3-18** from 30 µg /ml to 3.75 µg /ml is due to the decrease in the concentration of DPPH radical, which indicates the reduction capability of DPPH radicals by the antioxidant's activity. Therefore, oxidation-related diseases or free radicals can be prevented or treated with antioxidants that have the property of removing free radicals. [35] suggested that the presence of the pyrazole ring in coumarin showed promising DPPH radical scavenging activity and structure–activity relationship studies revealed that compounds containing electron-withdrawing groups/halogens showed good antioxidant properties.

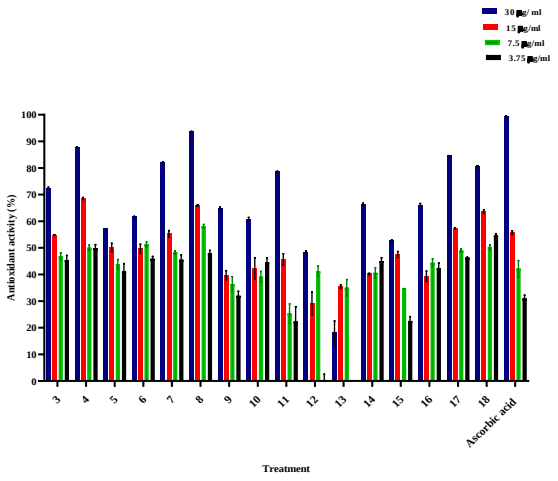

Figure. (2). DPPH radical Scavenging activity of compounds 3-18. Values are expressed as mean (n=3) of the percent inhibition of the absorbance of DPPH radicals.

Anticancer activity

The results of anticancer activity of the newly compounds against HepG-2, MCF-7 and HCT-116 cell lines indicated that the compounds at different concentrations affect the viability of the tested cell lines and the viability increased by decrease concentration (Figure 4). These results were summarized in table (3) and presented as the concentration of drug inhibition 50% cell growth (IC50). The IC_{50} of compound 18 was recorded 15.99 µg which indicated a strong anticancer activity against MCF-7 cell line (Table 3). It was observed that no compounds showed IC_{50} values lower than DOX against the tested human tumor cells. Notably, compounds **18** and **4** have significant cytotoxic activities against MCF-7 cell line.

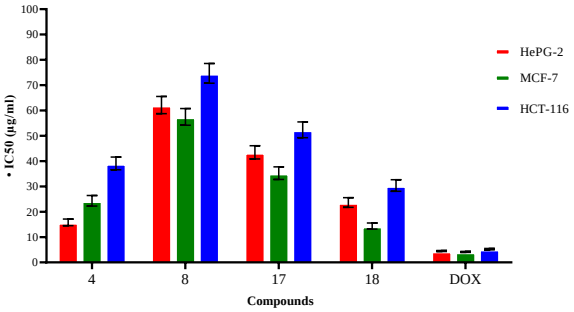

Figure (3). Cytotoxic activity of some compounds against human tumor cells. IC50 (µg/ml):1 – 10 (very strong). 11 – 20 (strong). 21 – 50 (moderate). 51 – 100 (weak and above 100 (non-cytotoxic).

Molecular docking study.

The docking simulations were conducted to assess the putative binding ability of the most promising anti-proliferative synthesized compounds **4, 8, 17,** and **18** with the VEGFR-2enzyme (PDB code: 4ASD). we used computational approaches to predict the inhibition potential of the most promising compounds **(4**, **8**, **17**, and **18**) to the growth factor receptor 2 (VEGFR-2) in comparison to sorafenib (PDB ID: 4ASD). Furthermore, the physicochemical and pharmacokinetic (ADMET) properties including were predicted**.**

In order to predict the potential of the most promising anti-proliferative synthesized compounds **(4**, **8**, **17** and **18)** to act as inhibitor for the VEGFR-2 enzyme molecular docking studies were performed. The docking studies were conducted within the active site of VEGFR-2 kinase (PDB ID: 4ASD). The binding site of VEGFR-2 kinase consist of a front binding pocket (ATP binding site) and hydrophobic back pocket that is an allosteric binding pocket [39, 40]. The important amino acids in the front pocket that contribute to the formation of H-bonds are Glu917, Cys919, and some inhibitors established H-bonds with Lys868, beside containing hydrophobic area made up of Leu840, Val848, Ala866, Lys868, Glu917, Phe918 and Gly922. While, the hydrophobic back pocket's important amino acids are Glu885, Asp1046, also, contains Ile888, Ile892, Val898, Val899, Leu1019, His1026, Ile1044, Cys1045, and Phe1047. The hydrophobic and Van Der Waals interactions are important in the inhibitors' binding affinity and selectivity [41,42].

Table (1). Antibacterial activity of compounds (**3 - 18**) against Gram-positive and Gram-negative bacteria in terms of the diameter of the inhibition zone diameter in mm [a]

Compounds	Test microorganisms					
	Gram +ve bacteria			Gram -ve bacteria		
	S. aureus	*B. cereus*	*L. monocytogen*	*E. coli*	*S. typhmirun*	*Y. enteroc*
3	8.5±0.07	10±2.19	8.5±0.035	--	13.5±0.21	11.5±0.07
4	14.5±0.07	13	12±0.14	10	15	13
5	14±0.14	13.5±0.035	11	15.5±0.07	12±0.14	16±0.14
6	15.5±0.35	13.5±0.11	--	13.5±0.21	14	--
7	15±0.14	13.5±0.04	13.5±0.04	13.5±0.07	12.5±0.07	9.5±0.07
8	15	14.5±0.18	14.5±0.11	14.5±0.35	15.5±0.35	18.5±0.21
9	12.5	14±0.07	13.55±0.1	16±0.35	14	15.5±0.07
10	12.5±0.07	13.5±0.12	12	13.5±0.14	--	10.5±0.07
11	13	12	14±0.07	15	14.5±0.07	15.5±0.070
12	10.5±0.07	11.5±0.035	17±0.035	11±0.14	--	14
13	15	10±0.21	13.5±0.32	10±0.43	--	14.5±0.070
14	16±0.14	13±0.14	17±0.18	13±0.28	12.5	13.5±0.070
15	15.5±0.07	14±0.14	12±0.18	13±0.43	12.5±0.35	--
16	11	14±0.07	14±0.21	16±0.14	14.5	--
17	13.5±0.07	12.5±0.18	11.5±0.12	13.5±0.21	--	10.5±0.070
18	15.5±0.070	15.5±0.32	17.5±0.18	15.5±0.64	17±0.35	14
R	22.5 ±1.0	18.5±0.035	16	15.5±0.070	16±0.141	15.5±0.07

The values (average of triplicate) are diameter of zone of inhibition at 1 mg/mL

Table (2). Antifungal activity of compounds (**3-18**) in terms of the diameter of the inhibition zone diameter in mm.

Compounds	Test microorganisms	
	Fusarium sp	*A. Niger*
3	--	--
4	--	11.75±(
5	--	12±1.42
6	--	--
7	--	--
8	30.5±070	14.75±0.35
9	10.75±1.06	10.5±0.70
10	12	--
11	--	10.75±0.35
12	14±0.70	15.5±0
13	18	13.5±2.
14	--	--
15	--	10.5±0.3
16	--	--
17	11.5±0.70	--

18	14.5±0.35	16.25±1.77
R	17±1.41	14.5±3.54

[a] The values (average of triplicate) are diameter of zone of inhibition at 1 mg/mL

Table (3): The IC50 of compounds (4, 8, 17, 8) in HepG-2 and MCF-7 and HCT-116 cell lines.

Compou no	IC_{50} (µg/ml)		
	HePG-	MCF-7	HCT-1
4	15.82±	24.34±	39.1±2
8	62.13±	57.48±	74.67±
17	43.46±	35.25±	52.36±
18	23.66±	14.36±	30.36±
DOX	4.50±0	4.17±0.	5.23±0

IC_{50} (µg/ml):1 – 10 (very strong). 11 – 20 (strong). 21 – 50 (moderate). 51 – 100 (weak and above 100 (non-cytotoxic)

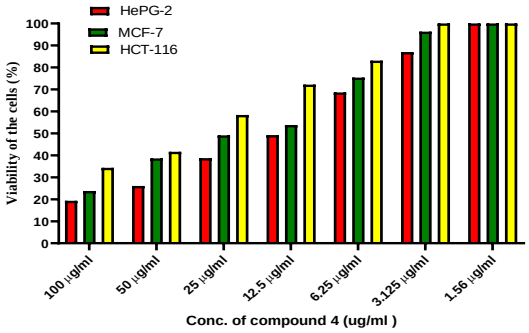

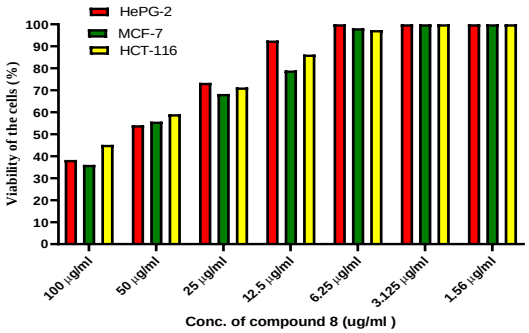

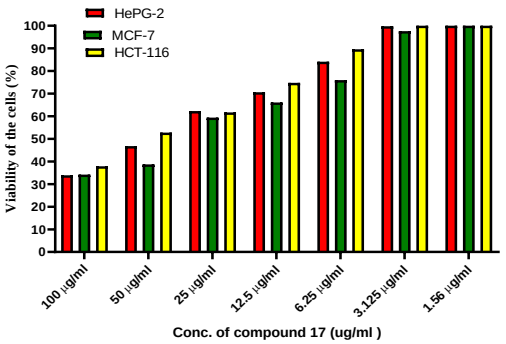

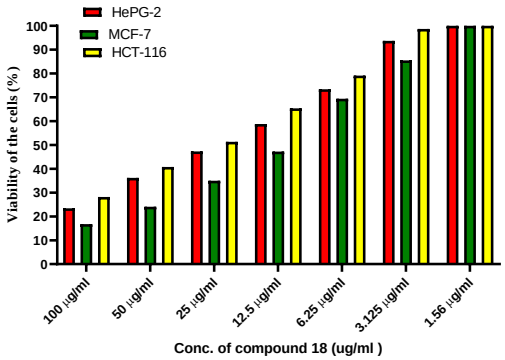

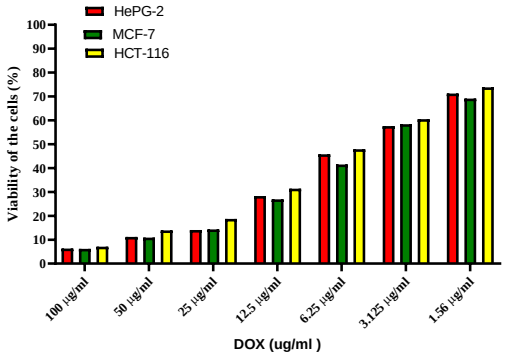

Figure 4. Dose dependent cytotoxicity for the tested compounds (4, 8, 17 and 18 and DOX) (conc. 100- 0 µg/ml) against HepG-2 and MCF-7 and HCT-116 cells.

The VEGFR-2 kinase inhibitors are categorized based on their binding positions: type I bind to the ATP site, type II bind to the ATP site as well as the hydrophobic back pocket and are more selective than type I inhibitors, and type III inhibitors bind wholly outside the ATP binding site, beyond the gatekeeper residue [43].

Our docking studies were performed within the active site of human VEGFR-2 protein (PDB code: **4ASD**) using the MOE 2019 program. The binding energy and type of interaction of new synthesized compounds **(4**, **8**, **17** and **18)** with the VEGFR-2 protein (PDB code: **4ASD**) were depicted in **Table 4**. At the begging, to validate our docking protocol, the co-crystallized ligand was re-docked into the enzyme active pocket. The co-crystallized ligand docking result showed That the root mean square deviation (RMSD) value between the native ligand and re-docked pose was too small (0.19 Å), which indicated the reliability of the docking protocol. The co-crystallized ligand showed docking score of −10.65 kcal mol^{-1} and formed H-bonds with the amino acid residues of the front and back pocket Cys919, Glu885, Asp1046, respectively beside pi-H interaction between phenyl ring and Lys868 and Asp1046 residues (**Table 4, Figure 5**). The docking results of the selected compounds showed better docking score with the

VEGFR-2 active site ranging from -6.43 to -8.89 kcal mol^{-1} and all of them were surrounded by the amino acids of the target protein with the formation of several H-bonds and hydrophobic interactions with the amino acid residues of the front and back pocket in similar manner as native ligand, sorafenib (**Table 4**)

Compound **4** revealed binding score of -6.43 kcal mol^{-1} and occupied the back pocket of the VEGFR-2 kinase by forming three H-bond donors with the amino acid Asp1046 in a good distance (**Table 4**). In case of compound **8**, the presence of 4-amino pyrimidine-2-thione moiety led to the better docking score of -7.78 kcal mol^{-1} than compound **4** and changed the orientation of **8** within the active site of VEGFR-2 kinase, forming interaction with the amino acids of the ATP binding site (front pocket). The N atom of pyrimidine ring acted as HBA and established three H-bonds with the NH of Lys868 residue (front pocket), while the phenyl ring attached to *N* atom of pyrazole ring produced three pi-H interaction with the same amino acid Lys868. Also, the sulfur atom plays a crucial part in the interaction by forming six H-bond acceptors with the Gly1048, Leu1049 (**Table 4, Figure 6**). The introduction of sugar moiety to the amino group of pyrimidine ring in compound **17** result in lowest binding energy of -8.89 kcal $mol^{-1}$and excellent binding mode with both the ATP binding pocket and the allosteric site. Three pi-H interaction with the Lys868 (front bocket) were established by the phenyl ring linked to N atom of the pyrazole ring. On the other, the OH groups act as HBD and HBA, forming nine H-bonds with the amino acidAsp814, His1026, Arg1027 (**Table 4, Figure 7**). In case of compound **18** with docking affinity of -7.10 kcal mol^{-1}, the amino acid Lys868 in the front pocket established one H-bond acceptor with the N atom of the pyrimidine ring and three pi-H interactions with the phenyl ring linked to the N of the pyrazole ring. In addition, the pyrazole ring produced three pi-H interaction with the Leu889 residue, while the 1,3-diazete-2(1H)-thione moiety introduced a new binding mode with the amino acids Glu885 and Asp814 (ionic interactions, **Table 4**).

Physicochemical and ADMET Prediction

The physicochemical and pharmacokinetic (ADMET) properties of compounds **4**, **8**,**17**, **18** and sorafenib were predicted according to Lipinski's rule of 5 using the free web-based tools *SwissADME* (http://www.swissadme.ch/index.php) *and pkCSM-pharmacokinetics* (http://biosig.unimelb.edu.au/pkcsm/), respectively. Lipinski's rule state that any ligand can be considered as a drug-like, if obey the following criteria: molecular weight<500 Dalton, number of H-bond donors<5, number of H-bond acceptors<10 and LogP<5 [46] .The results obtained demonstrated that compound **4** and sorafenib followed Lipinski's criterion. Compound **8** obeyed the rule of Lipinski in the terms of molecular weight, number of HBAs, and HBA groups, but exceeded the limit of *log P* value by 1.15 (**Table 5**). Although compound **17** had a lower *log p* value (2.99) than Sorafenib (4.05), but it violated two Lipinski's rule: the molecular weight exceeded the specified limit by 99 amu, and the number of HBA groups surpassed the limit by one. Furthermore, compound **18** breached two of Lipinski's rules: the log p value was 0.96 higher than the limited value, and no HBD groups were present (**Table 5**).

In addition, other set of physicochemical parameters were specified to promote drug likeness including topological polar surface area (TPSA $\leq$ 140), atomic molar refractivity between 40 to 130, and the number of rotatable bonds $\leq$ 10 [47]. All compounds as well as Sorafenib are in agreement with these criteria except compound **17** (**Table 5)**.

ADMET Prediction

The study of what happens to drugs when they are administered and pass through the body, including the absorption, distribution, metabolism, excretion, and toxicity (ADMET) properties, is known as pharmacokinetics [46]. The ADMET profile of compounds (**4**, **8**, **17**, **18**) and sorafenib were evaluated by *pkCSM* (http://biosig.unimelb.edu.au/pkcsm/).

The result indicates that, compound **8**, **17** were water soluble and compound **18** have better oral absorption than sorafenib. All compounds can be efficiently absorbed in the human intestine better than sorafenib except compound **17** and have comparable skin permeability (log Kp). Compounds **4**, **8**, and **18** have the capability to reach CNS (CNS permeability -1.373 to -1.713) higher than sorafenib (-2.02), while compound **17** was unable to penetrate (CNS permeability 4.0). Also, our result revealed that, compounds **(8** and **17)** were non-inhibitor for CYP1A2, CYP3A4 and CYP2D6 (**Table 5).**

Excretion was expected based on total clearance, which is an important factor in determining dosage intervals [47]. Unfortunately, the obtained data revealed that the four compounds demonstrated higher clearance rates than sorafenib. As a result, our compounds are expected to be excreted faster and with shorter dosage intervals (**Table 5**).

Toxicity is the final ADMET profile factor that has been investigated. Currently, toxicity is the leading cause of drug candidate failure in clinical trials [48]. **Table 5** illustrates the four studied compounds **(4**, **8**, **17** and **18)** demonstrated the lowest tolerated doses (0.373 - 0.415 log mg/kg/day) than sorafenib of 0.73

(log mg/kg/day). The oral acute toxic doses (LD_{50}) of the new compounds were slightly higher (2.756-2.935) than sorafenib (2.545). While, compounds (**4** and **18**) revealed very low chronic toxicity of 0.261 and -0.264 (log mg/kg_bw/day) than sorafenib of 0.889 (log mg/kg_bw/day) and only compound **4** was anticipated to be non-hepatotoxic. Finally, compounds **4** and **18** had lower Minnow toxicity values of -1.798 and -1.976 in contrast to sorafenib of 0.385, indicating that they are more selective towards cancer cells than normal cells (**Table 5)**.

We used molecular docking, ADMET and drug likeness analysis to examine the potential of most promising anti-proliferative synthesized compounds **(4, 8, 17,** and **18)** to act as VEGFR-2 inhibitors. Overall results proposed that, compounds **(8, 17,** and **18)** had the lowest binding energies ranging from -7.10 to -8.89 kcal/mol and developed a strong binding mode with both the ATP binding pocket and the allosteric site of the VEGFR-2 enzyme (PDB code: 4ASD). Furthermore, the selected compounds represented good *in silico* ADMET prediction.

Table 4: Molecular docking result of new synthesized compounds (4, 8, 17 and 18) within the VEGFR-2 active pocket (PDB ID:4ASD)

Comp. N	Score Kcal/mo	Moieties from the com	Amino residues	Type of interaction, Distance Å
Sorafeni	-10.65	NH	Glu885	H-donor 2.65, 2.93, 2.97, 3.13
	RMSD: Å	CO	Asp104(	H-acceptor 2.88, 2.88
		NH	Cys919	H-acceptor 3.53, 3.53
		Phenyl ring	Lys868	pi-H4.26, 4.28
		Phenyl ring	Asp104(	pi-H 4.04, 4.05
4	-6.43	CH	Asp104(	H-donor 2.89, 3.16, 2.62
8	-7.78	N of pyrimidine ring	Lys868	H-acceptor 2.90,3.03, 3.06
		S	Gly104	three H-acceptor 4.18
		S	Leu104	three H-acceptor 4.37
		Phenyl ring	Lys868	pi-H 3.62, 3.63, 3.81
17	-8.89	OH	Asp814	H-donor 2.60, 2.71
		OH	His1026	three H-donor 2.96
		OH	Arg102	H-acceptor 3.01, 2.94, 2.96, 3.06
		Phenyl ring	Lys868	pi-H 3.65, 3.67, 3.82
18	-7.10	N of pyrimidine ring	Lys868	H-acceptor3.31
		N of diazete ring	Glu885	Ionic 4.00
		N of diazete ring	Asp814	Ionic 3.86, 3.89
		Phenyl ring	Lys868	pi-H 3.64, 3.66, 3.80
		Pyrazole ring	Leu889	pi-H 4.13, 4.27, 4.07

Table 5. ADMET profile of the four most active compounds **(4**, **8**, **17**, **18**, and **sorafenib)**

Parameters (unite)	**4**	**8**	**17**	**18**	**Sorafenib**
Physicochemical Property					
Molecular weight (g/mol)	424.88	483.97	599.047	493.97	464.82
Log *P*	4.60	5.15	2.99	5.18	4.05
Num. rotatable bonds	3	3	8	3	9
No. H-acceptors	3	3	9	4	7
No. H-donors	1	2	5	0	3
TPSA (Å²)	76.86	113.84	162.00	140.69	92.35
Molar Refractivity	119.44	135.41	159.16	89.32	112.48
Absorption					
Log S (log mol/L)	-6.54	-3.08	-3.145	-6.122	-3.96
Caco2 permeability (log Papp in 10^{-6} cm/s)	0.518	0.776	-0.529	1.262	0.903
Human Intestinal absorption (%)	98.324	97.783	65.974	94.62	92.83
Skin permeability	-2.731	-2.735	-2.735	-2.734	-2.74
P-glycoprotein substrate	Yes	Yes	Yes	Yes	Yes
P-glycoprotein I inhibitor	Yes	No	No	Yes	Yes
P-glycoprotein II inhibitor	Yes	Yes	Yes	Yes	Yes

Distribution					
VDss (log L/kg)	-0.198	-1.147	-1.085	0.051	-0.242
BBB permeability (log BB)	-0.612	-1.566	-1.893	-0.029	-1.71
CNS permeability (log PS)	-1.557	-1.713	-4.004	-1.373	-2.022
Metabolism					
CYP2D6 substrate	No	No	No	No	No
CYP3A4 substrate	Yes	Yes	Yes	Yes	Yes
CYP1A2 inhibitor	Yes	No	No	No	Yes
CYP3A4 inhibitor	Yes	No	No	Yes	Yes
CYP2C19 inhibitor	No	Yes	No	Yes	Yes
CYP2C9 inhibitor	Yes	Yes	Yes	Yes	Yes
CYP2D6 inhibitor	No	No	No	No	No
Excretion					
Total clearance	0.142	0.186	0.652	0.282	-0.219
Renal OCT2 substrate	No	No	No	No	NO
Toxicity					
Human max. tolerated dose ml/min/kg)	0.415	0.443	0.435	0.373	0.73
Oral rat acute toxicity (LD50, mo	2.935	2.756	2.943	2.846	2.545
Oral Rat Chronic Toxicity mg/kg_bw/day)	0.261	1.989	4.60	-0.264	0.889
hERG I inhibitor	No	No	No	No	No
hERG II inhibitor	Yes	Yes	Yes	Yes	Yes
Hepatotoxicity	No	Yes	Yes	Yes	Yes
Skin sensitization	No	No	No	No	NO
T.Pyriformis toxicity (log ug/L)	0.287	0.285	0.285	0.286	0.376
Minnow toxicity (log mM)	-1.798	2.967	2.937	-1.976	0.385

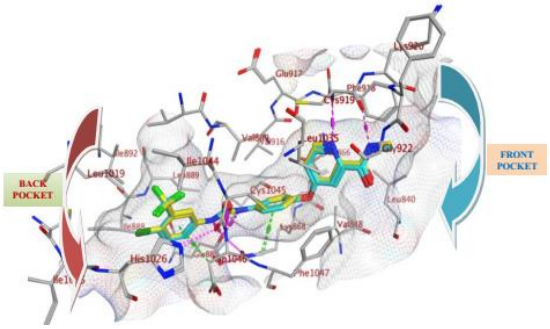

Figure 5. 3DBinding mode of the re-docked ligand (yellow, stick) within VEGFR-2 active pocket (PDB ID:4ASD) showed that it was superimposed on the same position as the native ligand (cyan, stick)

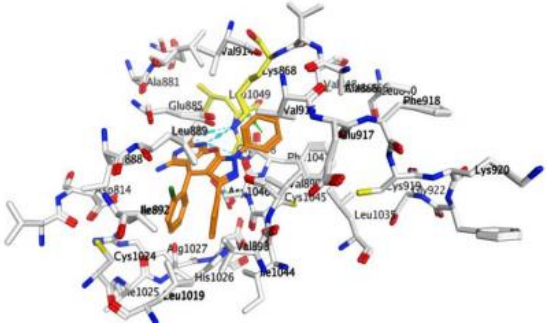

Figure 6. 3D Binding mode of compound 8 (brown, stick) within VEGFR-2 active pocket (PDB ID: 4ASD).

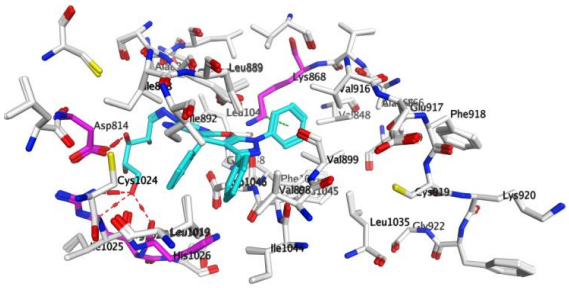

Figure 7. 3D Binding mode of compound **17** (cyan, stick) within VEGFR-2 active pocket (PDB ID: 4ASD).

5. CONCLUSION

Novel Pyrano[2,3-c]pyrazole and their sugar derivatives were synthesized in good yields. The structures of the new compounds were elucidated by different elemental and spectral analyses. The study of the biological activity revealed that compound **18** exhibited promising antibacterial activity against *L. monocytogenes* and *S. typhmirum* (17.5, 17 mm, respectively) comparing to cefoperazone (16 mm). Moreover, it was active against *E. coli* (15.5 mm) and *Y. enterocolitica* (14 mm) and exhibited a strong anticancer activity against MCF-7 cell line. Furthermore, compound **8** showed a potent activity against *Y. enterocolitica* strain (18.5 mm) and displayed excellent antifungal activity against *Fusarium sp.* Compound 8 showed excellent

scavenging activity at all tested concentrations. A molecular docking study illustrated the potency of compounds 8 and 18 as potential bioactive compounds.

.

CONFLICT OF INTEREST

There is no conflict of interest.

References

1. El-Arab, E. E. Synthesis and cytotoxicity of novel pyrazole derivatives derived from 3-methyl-1-phenyl-1H-pyrazol-5 (4H)-one. Egyptian Journal of Chemistry, 58, 741-53. (2015).
2. Khafagy, M. M.; Abd El-Wahab, A. H.; Eid, F. A.; El-Agrody, A. M.; Synthesis of halogen derivatives of benzo [h] chromene and benzo [a] anthracene with promising antimicrobial activities. Il Farmaco, 57, 715-722. (2002).
3. Kumar, D.; Reddy, V. B.; Sharad, S.; Dube, U.; Kapur, S. A facile one-pot green synthesis and antibacterial activity of 2-amino-4H-pyrans and 2-amino-5-oxo-5, 6, 7, 8-tetrahydro-4H-chromenes. European Journal of Medicinal Chemistry, 44, 3805-3809 (2009).
4. Konkoy, C. S.; Fick, D. B.; Cai, S. X.; Lan, N. C.; Keana, J. F. U.S. Patent No. 6,680,332. Washington, DC: U.S. Patent and Trademark Office. (2004).
5. Bansal, R. K. Heterocyclic chemistry. New Age International. (2008).
6. Abdelrazek, F. M.; Metz, P.; Jäger, A.; Metwally, N. H. An Eco-friendly Synthesis of Some Novel 4-methyl-4-hetaryl Chromene and Pyrano [2, 3-c] pyrazole Derivatives. Journal of Heterocyclic Chemistry, 54, 2313-2318 (2017).
7. Babaie, M.; Sheibani, H. Nanosized magnesium oxide as a highly effective heterogeneous base catalyst for the rapid synthesis of pyranopyrazoles via a tandem four-component reaction. Arabian Journal of Chemistry, 4, 159-162. (2011).
8. Foloppe, N.; Fisher, L. M.; Howes, R.; Potter, A.; Robertson, G. S.; Surgenor, A. E. Identification of chemically diverse Chk1 inhibitors by receptor-based virtual screening Bioorg. Med. Chem., 14, 4792- 4802 (2006).
9. Litvinov, Y. M.; Shestopalov,A. A.; Rodinovskaya, L. A. ; Shestopalov , A. M. New convenient four-component synthesis of 6-amino-2,4-dihydropyrano [2,3-c]pyrazol-5-carbonitriles and one-pot synthesis of 6'-aminospiro[(3H)-indol-3,4'-pyrano[2,3-c]pyrazol]-(1H)-2-on-5'-carbonitriles. J. Comb. Chem., 11, 914–919 (2009).
10. Kshirsagar, S. W.; Patil, N. R.; Samant,S. D. Mg-Al Hydrotalcite as a First Heterogeneous Basic Catalyst for the Synthesis of 4H-Pyrano[2,3-c]pyrazoles Through a Four-Component Reaction Synth. Commun., 41, 1320–1325 (2011).
11. Reddy, M. B. M.; Jayashankara,V. P. ; Pasha ,M. A. Glycine-catalyzed efficient synthesis of pyranopyrazoles via one-pot multicomponent reaction Synth. Commun., 40, 2930–2934 (2010).
12. Khurana, J. M.; Nand ,B. ; Kumar ,S. Rapid Synthesis of Polyfunctionalized Pyrano[2,3-c]pyrazoles via Multicomponent Condensation in Room-Temperature Ionic Liquids Synth. Commun., 41, 405–410 (2011).
13. Peng, Y.; Song, G.; Dou, R.. Surface cleaning under combined microwave and ultrasound irradiation: Flash synthesis of 4 H-pyrano [2, 3-c] pyrazoles in aqueous media Green Chem., 8, 573–575 (2006).
14. Sharanina ,L. G.; Promonenkov, L. G.;Puzanova ,V. V. ; Sharanona ,Y. A. 6-Amino-5-cyano-1H, 4H-pyrazolo [3, 4-b] pyrans Chem. Heterocycl. Compd., 18, 607–611 (1982).
15. Heravi, M. M.; Beheshtiha ,Y. S.; Pirnia, Z.; Sadjadi ,S.; Adibi .M. Synth. Commun., 39, 3663–3667 (2009).
16. Valizadeha ,H.; Azimib, A. A. ZnO/MgO containing ZnO nanoparticles as a highly effective heterogeneous base catalyst for the synthesis of 4H-pyrans and coumarins in [bmim] BF4 J. Iran. Chem. Soc., 8, 123–130 (2011).
17. Maleki, A.; Taheri-Ledari,R.; Rahimi, J.; Soroushnejad, M.; Hajizadeh ,Z. Facile Peptide Bond Formation: Effective Interplay between Isothiazolone Rings and Silanol Groups at Silver/Iron Oxide Nanocomposite Surfaces ACS Omega, 4, 1062939 (2019).
18. Maleki, A.; Taheri-Ledari,R.; Rahimi, J.; Soroushnejad, M.; Hajizadeh ,Z. Novel biocompatible core/shell Fe3O4@NFC@Co(II) as a new catalyst in a multicomponent reaction: an efficient and sustainable methodology and novel reusable material for one-pot synthesis of 4H-pyran and pyranopyrazole in aqueous media ACS Omega, 2019, 4, 1062939 .Maleki,A. Polycyclic Aromatic Compounds., 38,402–409 (2018).
19. Abu-Dief, A. M.; Nassar, I. F.; El Sayed, W. H.; Magnetic NiFe2O4 nanoparticles: efficient, heterogeneous and reusable catalyst for synthesis of acetylferrocene chalcones and their anti-tumour activity Appl. Organometal. Chem., 30, 917 (2016).
20. Nassar, I. F.; El Farargy, A. F.; Abdelrazek, F. M.; Ismail, N. S. M. Design, Synthesis and Anticancer Evaluation of Novel Pyrazole,

Pyrazolo[3,4-d] Pyrimidine and Their Glycoside Derivatives, Nucleosides, Nucleotides and Nucleic Acids, 36:4, 275 (2017).
21. Nassar, I. F.; El Farargy, A. F.; Abdelrazek, F. M. Synthesis and Anti-Cancer Activity of Some New Fused Pyrazoles and Their Glycoside Derivatives J heterocyclic chem., 55, 1709 (2018).
22. Nassar, I. F.; Att-Allah,S. R.; Hemdan, M. M. Utility of Thiophene-2-carbonyl isothiocyanate as a synthon of 1,2,4-Triazole, 1,3.4-Oxadiazole and 1,3.4-Thiadiazole derivatives with evaluation of their Antitumor and Antimicrobial activities. phosphorous, sulphur and silicon, 193, 630-636 (2018).
23. Abdel Rahman, A. A. H.; Shaban, A. K. F.; Nassar, I. F.;Yousif, M. N. M.;EL-Kady ,D. S.; Awad, H. M.; El-Sayed ,W. A. Synthesis and Anticancer Activity of New Pyrimidine and Oxadiazole Acyclic Nucleoside Analogs and Thiazolopyrimidine Derivatives Russian Journal of General Chemistry, 91, 2086–2094 (2021).
24. Atta-Allah, S.R.; Ismail, S.M.; Nassar, I. F.; Design, Synthesis and Anti-inflammatory Activity of Novel 5-(Indol-3-yl)-thiazolidinone Derivatives as COX-2 Inhibitors. Letters in Drug Design & Discovery, 18,525 – 541 (2021).
25. Abdel Rahman, A .A. H.; Shaban ,A.K. F.; Nassar I. F.; EL-Kady.D. S.; Ismail ,M. S.; Mahmoud, S. F.; Awad ,H.M.; El-Sayed, W. A. Discovery of New Pyrazolopyridine, Furopyridine and Pyridine Derivatives as CDK2 inhibitors: Design, Synthesis, Docking studies, and Anti-proliferative Activity Molecules,26,3923 (2021).
26. Lashin, W.; Nassar, I. F.; El Farargy, A. F.; Osman, A. O. Synthesis of New Furanone Derivaties with Potent Anti-Cancer Activity Russian Journal of Bioorganic Chemistry, 46, 1074–1086 (2020).
27. Elewa, S, I.; Mansour, E; Nassar, I. F.; Mekawey, A. A. I. Synthesis of Some New Pyrazoline Based Thiazoles Derivatives and Evaluation of their Antimicrobial, Antifungal and Anticancer Activities Russian Journal of Bioorganic Chemistry, 46, 382–392 (2020).
28. Nassar, I. F.; El Farargy A. F.; Abdelrazek F. M.; Hamza, Z. Synthesis of New Uracil Derivatives and Their Sugar Hydrazones with Potent Antimicrobial, Antioxidant and Anticancer Activities Nucleosides, Nuclesotides and nucleic Acids, 39, 991–1010 (2020).
29. Nassar I. F.; EL-Kady, D. S.; Awad, H. M.; El-Sayed ,W. A. Design, Synthesis and Anticancer Activity of New Oxadiazolyl- and Thiazolyl-linked Benzoimidazole Arylidines, Thioglycoside and Acyclic Analogs J Heterocyclic Chem.,56, 1086 (2019).
30. Nassar, I. F.; El-Sayed, W. A.; Ragab, T.I.; Shalaby A, S, G.; Mehany ,A. Design, Synthesis of Novel Pyridine and Pyrimidine Sugar Compounds as Antagonists Targeting the ERα via Structure-Based Virtual Screening mini reviews in medicinal chemistry., 19, 395 – 409 (2019).
31. Abdel Rahman, A. A.H.; Nassar, I. F., Shaban, A. K. F.; El Sayed.W.A.; Synthesis, Docking Studies and Anticancer Activity of Novel Pyrimidine Compounds and Their Glycoside Derivatives. Mini Reviews in Medicinal Chemistry., **19,**1093-1110 **(2019).**
32. Abdel-Rahman T. M.; El-Hashash M. A.; Nassar I. F.; "Synthesis of Heterobicyclic Quinazolinones Derived From N-[2-(2-chloro-phenyl)-1-(6,8-dibromo-4-oxo-4H-benzo[d][1,3]oxazin-2-yl)-vinyl]benzamide as Anti-microbial Agents; Egypt. J. Chem. 49, No. 4, pp. 461-474 (2006).
33. Kassem ,A. F.; Nassar, I.F.; Abdel Aal, M. T.; Awad, H. M.; El-Sayed ,W.A.; Synthesis and Anticancer Activity of New ((Furan-2-yl)-1,3,4-thiadiazolyl)-1,3,4-Oxadiazole Acyclic Sugar Derivatives; Chemical and Pharmaceutical Bulletin Japan Chem. Pharm. Bull. 67, 888–895 (2019).
34. Abu-Melha, S. Design, synthesis and DFT/DNP modeling study of new 2-amino-5-arylazothiazole derivatives as potential antibacterial agents. Molecules, 2018, 23,434.
35. Kenchappa, R.; Bodke, Y. D.; Chandrashekar, A.; Sindhe, M. A.; Peethambar, S. K. Synthesis of coumarin derivatives containing pyrazole and indenone rings as potent antioxidant and antihyperglycemic agents. Arabian Journal of Chemistry, 2017,10, S3895-S3906.
36. Brand-Williams, W.; Cuvelier, M, E.; Berset, C. L. W. T. Use of a free radical method to evaluate antioxidant activity. LWT-Food science and Technology, 28,25-30 1995,
37. Mosmann, T. Rapid colorimetric assay for cellular growth and survival: application to proliferation and cytotoxicity assays. Journal of immunological methods, 65, 55-63 (1983).
38. McTigue, M.; Murray, B. W.;Chen, J. H.; Deng, Y. L.; Solowiej, J.; Kania, R. S. Molecular conformations, interactions, and properties associated with drug efficiency and clinical performance among VEGFR TK inhibitors. Proceedings of the National Academy of Sciences, 109, 18281-18289 (2012)

39. Liu, Y.; Gray, N. S. Rational design of inhibitors that bind to inactive kinase conformations. Nature chemical biology, 2, 358-364 (2006).
40. Mohamed, T. K.; Batran, R. Z.; Elseginy, S. A.; Ali, M. M.; Mahmoud, A. E. Synthesis, anticancer effect and molecular modeling of new thiazolylpyrazolyl coumarin derivatives targeting VEGFR-2 kinase and inducing cell cycle arrest and apoptosis. Bioorganic chemistry, 85, 253-273 (2019).
41. Bauer, D.; Whittington, D. A.; Coxon, A.; Bready, J.; Harriman, S. P.; Patel, V. F.; Harmange, J, C. Evaluation of indazole-based compounds as a new class of potent KDR/VEGFR-2 inhibitors. Bioorganic & medicinal chemistry letters, 18, 4844-4848 (2008).
42. Honda, T.; Nagahara, H.; Mogi, H.; Ban, M.; Aono, H. KDR inhibitor with the intramolecular non-bonded interaction: Conformation–activity relationships of novel indole-3-carboxamide derivatives. Bioorganic & medicinal chemistry letters, 21, 1782-1785. 2011,
43. Wu, X.; Wan, S.; Wang, G.; Jin, H.; Li, Z.; Tian, Y.; Zhang, J. Molecular dynamics simulation and free energy calculation studies of kinase inhibitors binding to active and inactive conformations of VEGFR-2. Journal of Molecular Graphics and Modelling, 56, 103-112 (2015).
44. Lin, L. T.; Hsu, W. C.; Lin, C. C. Antiviral natural products and herbal medicines. Journal of traditional and complementary medicine, 4, 24-35 (2014).
45. Cheng, F.; Li, W.; Zhou, Y.; Shen, J.; Wu, Z.; Liu, G.; Tang, Y. A Comprehensive Source and Free Tool for Assessment of Chemical ADMET Properties, ACS Publication Chem. Inf. Model. 52, ,3099–3105 (2012).
46. Aluwi, M. F. F. M.; Rullah, K.; Yamin, B. M.; Leong, S. W.;Bahari, M. N. A.; Lim, S. J.; Lam, K. W. Synthesis of unsymmetrical monocarbonyl curcumin analogues with potent inhibition on prostaglandin E2 production in LPS-induced murine and human macrophages cell lines. Bioorganic & medicinal chemistry letters, 26, 2531-2538 (2016).
47. Abdelgawad, M. A.; El-Adl, K.; El-Hddad, S. S.; Elhady, M. M.; Saleh, N. M.; Khalifa, M. M.; Abd El-Sattar, N. E. Design, Molecular Docking, Synthesis, Anticancer and Anti-Hyperglycemic Assessments of Thiazolidine-2, 4-diones Bearing Sulfonylthiourea Moieties as Potent VEGFR-2 Inhibitors and PPARγ Agonists. Pharmaceuticals, 15, 226 (2022).
48. Rashid, U.; Hassan, S. F.; Nazir, S.; Wadood, A.; Waseem, M.; Ansari, F. L. Synthesis, docking studies, and in silico ADMET predictions of some new derivatives of pyrimidine as potential KSP inhibitors. Medicinal Chemistry Research, 24, 304-315 (2015).

.